DNA Stretching and Immobilization through the Air/Water Dewetting Process

Wei-Ching Liao and Xin Hu
Department of Mechanical Engineering
Weixiong Wang and L. James Lee
Department of Chemical and Biomolecular Engineering
The Ohio State University, USA
Chung-Hsun Lin and Shiu-Wu Chau
Department of Mechanical Engineering
Chung Yuan University, Taiwan

Introduction

Recently, a molecular-combing based technique was developed to generate highly-ordered DNA nanowires.[1] In this method, a droplet of DNA solution is dropped on a glass coverslip and a PDMS stamp with microwells array is then pressed on the DNA solution. After the press, a peeling of PDMS stamp is performed to generate the dewetting of the DNA solution. Finally, highly ordered DNA wires can be observed on the PDMS stamp. In this study, the simulation work is carried out to understand why DNA and how DNA molecules are stretched and immobilized on the PDMS substrate. The free surface flow field is obtained by solving the fluid mechanics governing equations based on the finite volume discretization. The air-water interface is traced by the volume-of-fraction method. From the simulation results, when the air-water interface is dewetting over the well, the flow patterns computed will contribute the stretching and immoboliztion of DNA molecules.

Problem illustration

In Figure 1, the experimental work developed to create ordered DNA nanowires is shown. Basically, a PDMS stamp with a microwells array is pressed on a glass coverslip with a 20 μg/ml λ-DNA TE buffer solution (10 mM tris-HCl and 1 mM EDTA, pH = 8) droplet on it. DNA is incubated with YOYO-1 fluorescent dye at a dye-base pair ratio of 1:5. The micorwell array has 5 μm in diameter, 10 μm in center-to-center distance, and 4 μm in depth.

To simulate the physical peeling process, the problem is simplified to be an inversed way where the PDMS well is on the bottom and a flat glass in moving upward with a velocity of 5 m/s. Also, the computational domain is focused on a 3 by 3 microwell array. Within this 3 by 3 section, consider the PDMS stamp as flat surface is reasonable. Based on Figure 2, the boundary conditions on the left and right are the given atmosphere pressure, the top and bottom are the no-slip walls except that the top is a moving wall, and the other two sides are symmetric. Because of the top moving wall, a deforming body-fitted grid is used and updated at every time step. The integral form governing equations of a control volume in the problems are as follows:

$$\frac{\partial}{\partial t}\int_V \rho \mathrm{d}V + \int_S \rho(\mathbf{v} - \mathbf{v}_s) \cdot \mathbf{n}\mathrm{d}S = 0 \qquad\qquad (1)$$

$$\frac{\partial}{\partial t}\int_V \rho \mathbf{v}\,\mathrm{d}V + \int_S \rho \mathbf{v}(\mathbf{v}-\mathbf{v}_S)\cdot \mathbf{n}\,\mathrm{d}S = \int_S (\mathbf{f}\cdot\mathbf{n})\,\mathrm{d}S + \int_V \rho \mathbf{b}\,\mathrm{d}V \qquad (2)$$

$$f_i = \mu\left(\frac{\partial u_i}{\partial x_j}+\frac{\partial u_j}{\partial x_i}\right)e_j + pe_i + f_i^{\sigma} \qquad (3)$$

$$\frac{\partial}{\partial t}\int_V \mathrm{d}V + \int_S \mathbf{v}_S \cdot \mathbf{n}\,\mathrm{d}S = 0 \qquad (4)$$

$$\frac{\partial}{\partial t}\int_V c\,\mathrm{d}V + \int_S c(\mathbf{v}-\mathbf{v}_S)\cdot \mathbf{n}\,\mathrm{d}S = 0 \qquad (5)$$

, where the control volume V is bounded by a closed surface S with outward normal vector $\mathbf{n}$, and $\mathbf{v}$ denotes the flow velocity, $\mathbf{v}_S$ the surface velocity of S, ρ the fluid density, t the time, $\mathbf{f}$ the external force acting on S, and $\mathbf{b}$ the gravitational acceleration. The surface force $\mathbf{f}$ is computed by (3), where where e_i is the unit vector in the direction of Cartesian coordinate i, μ the fluid viscosity, p the pressure, and f_i^{σ} denotes the surface tension component in the direction of e_i. $\mathbf{v}_S$ is then determined by (4) and the flow front position is described by (5), where the volume fraction of fluid is defined as c, i.e. $c = 1$ for cells are filled by liquid, $c = 0$ for cells by air, and the case of $0 < c < 1$ for cells by both fluids.
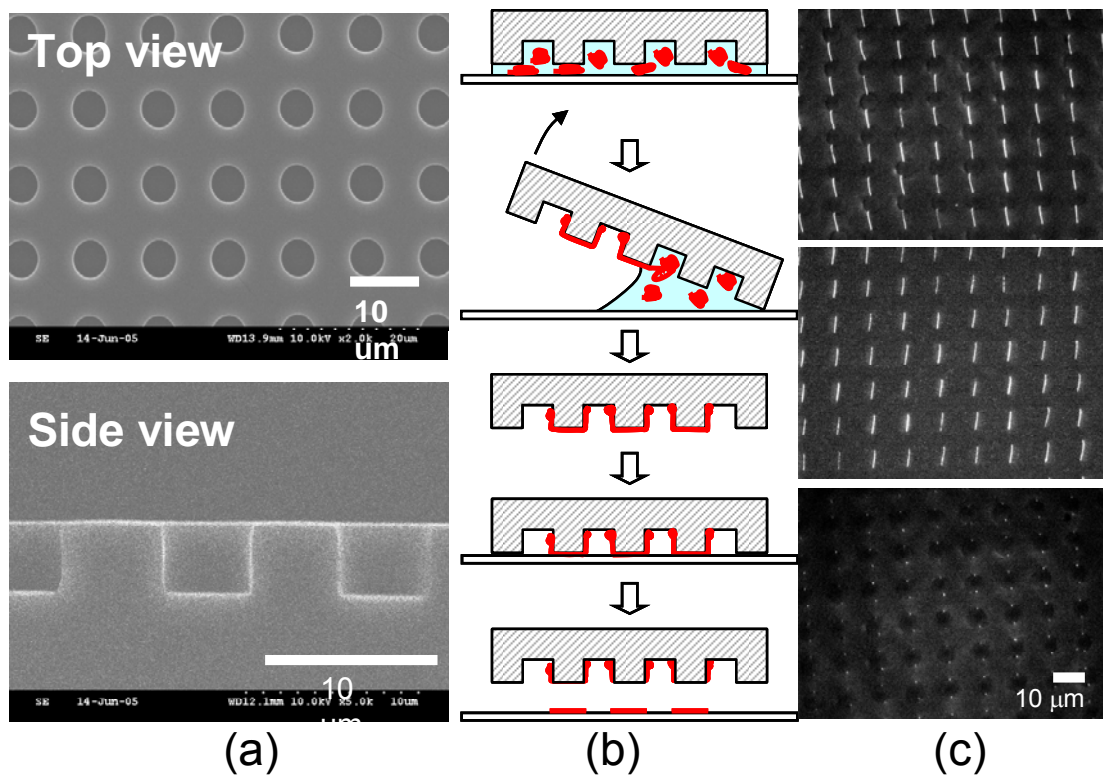
Figure 1. (a) The top and side view of PDMS microwell array. (b) The schematic description of generating DNA naostrands by peeling and transfer printing techniques. (c) Fluorescence micrographs of the original DNA nanostrands on PDMS stamp (top), the DNA nanostands on glass after transfer printing (middle) and the DNA nanostand ends remaining on PDMS stamp after transfer printing (bottom).[1]
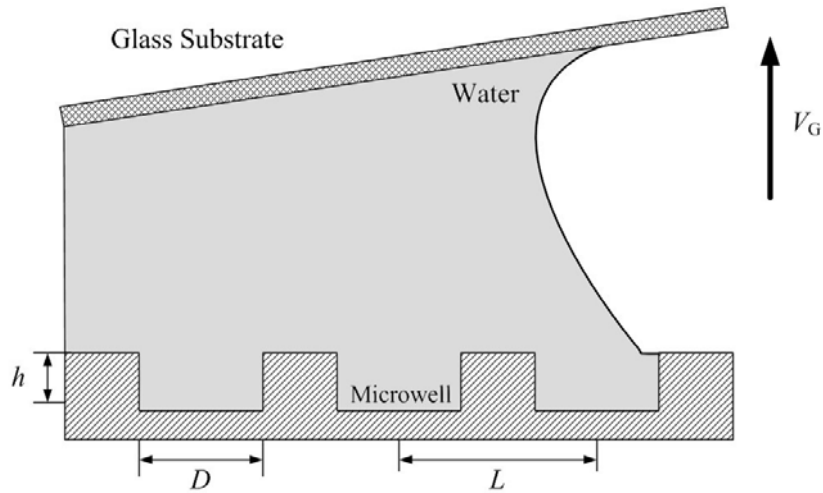
Figure 2. The schematic description of the problem to simulate

Simulation of the free surface flow is carried out by a finite volume method [2] based continuum mechanics solver COMET. About the free surface profile tracing, the scalar function c as in (5) is used to define the fluid as water (c = 1) and air (c = 0). Therefore, the free surface profile is implicitly define as c = 0.5 by solving (5) along with other governing equations. The determination of the surface tension follows the continuum surface force approach [3]:

$$\mathbf{f}^{\sigma} = -\sigma \left[\nabla \cdot \left(\frac{\nabla c}{|\nabla c|} \right) \right] \nabla c \qquad (6)$$

In addition, the physical properties of the fluid are summarized in Table 1.

Table 1. The physical properties of air and deionized water

Water density (kg/m^3)		998.3
Air density (kg/m^3)		1.188
Surface tension (N/m)		0.074
Contact angle (°)	Glass	34.3
	PDMS	112
Water viscosity (N·s/m^2)		1.002×10^{-3}
Air viscosity (N·s/m^2)		1.824×10^{-5}

Results and Discussions

Figure 3 depicts the predicted flow details inside the microwell at the peeling angle of 0°. Figure 3(a) gives the velocity vector of water at a vertical plane, where the red region denotes the air region and the blue one represents the space occupied by water. In following figures, the moving direction of the dewetting process is always from left to right. The water layer above microwell shows a consistent fluid tendency flowing to the left. A velocity gradient in vertical direction is clearly found at the left edge of the microwell. This gradient, as proposed in our previous study [1], should lead to partial uncoiling of DNA located in the region. The simulation reveals a strong downward flow near the detaching point shortly before the moving water front leaves this microwell. This downward flow should contribute to the uncoiling and immobilization of DNA at the left edge of the microwell. Figure 3(b) shows the velocity vector of water at a horizontal plane, where the blue region shows the free surface of water viewing from top. It indicates that a back flow, opposite to the front movement direction, occurs shortly before the detachment of the investigated microwell at the horizontal plane, as well as at the vertical plane shown in Figure 3(a). The strong back flow occurring inside microwells should explain the uncoiling and immobilization of DNA at the left edge of the microwell. Similarly, the immobilization of DNA at the right edge of the microwell can be understood by tracking the local flow motion near the right edge, where the fluid during the dewetting process flows almost parallel to the right vertical edge helping DNA ends to be attached on solid wall. In this way, the DNA nanostrands are immobilized between two neighboring microwells at their edges deep along the depth direction, which explains the immobilization mechanism of DNA nanostrand observed at microwell edges given in Figure 1.

(a)　　　　　　　　　　　　　　　　(b)
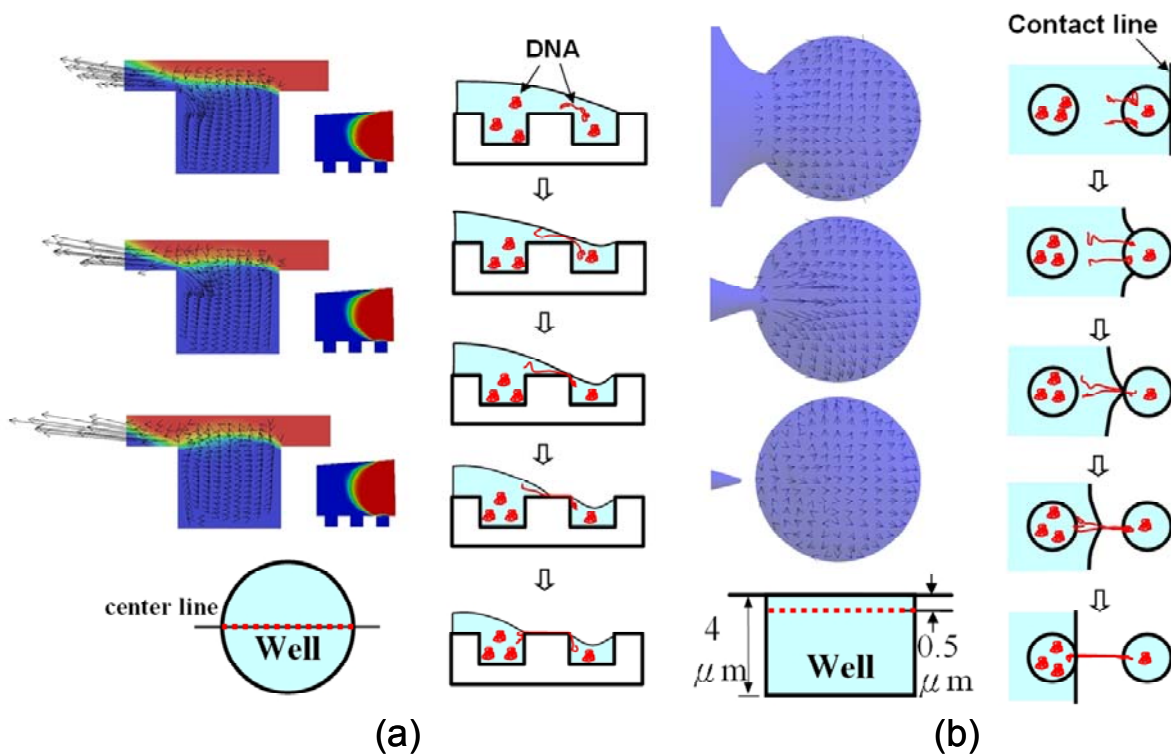
Figure 3. (a) The velocity vectors of the central vertical plane in the well. (b) The velocity vectors of a horizontal plane in the well.

Figure 4 illustrates time evolutions of water front moving among successive microwells, which helps to understand the stretching path between two neighboring microwells. Again, the blue surface indicates the location of water front. As proposed in our model [1] that the water front should have a dominant contribution to the pattern of DNA nanostrands between two microwells, we find that at the studied peeling angle (e.g. $\theta=0°$) the water front gives a tail-like region connecting to the previous microwell, before it completely detaches from the previous microwell. This tail-like water front seems to sustain its shape for some time instance and gradually vanishes, as it approaches the next neighboring microwell. The sharp shape of water front obviously contributes to cluster and locate DNA nanostrands at that location, especially for those DNA nanostrands already having one end immobilized at the left edge of previous microwell. This unique feature of dewetting behavior between microwells generates a distinctive DNA array pattern between two successive microwells, where the DNA nanostrands automatically and principally align along the peeling direction, not perpendicular to the front moving direction. Because the deformation and movement of water front mainly depends on the relative position of the water front land neighboring microwells (suppose the peeling velocity varies little in the experiments), the behavior of tail-like water front is therefore significantly influenced by the peeling angle. By tracking the peak location of the tail-like water front, the trajectory of DNA nanostrands connecting neighboring microwells can be predicted.
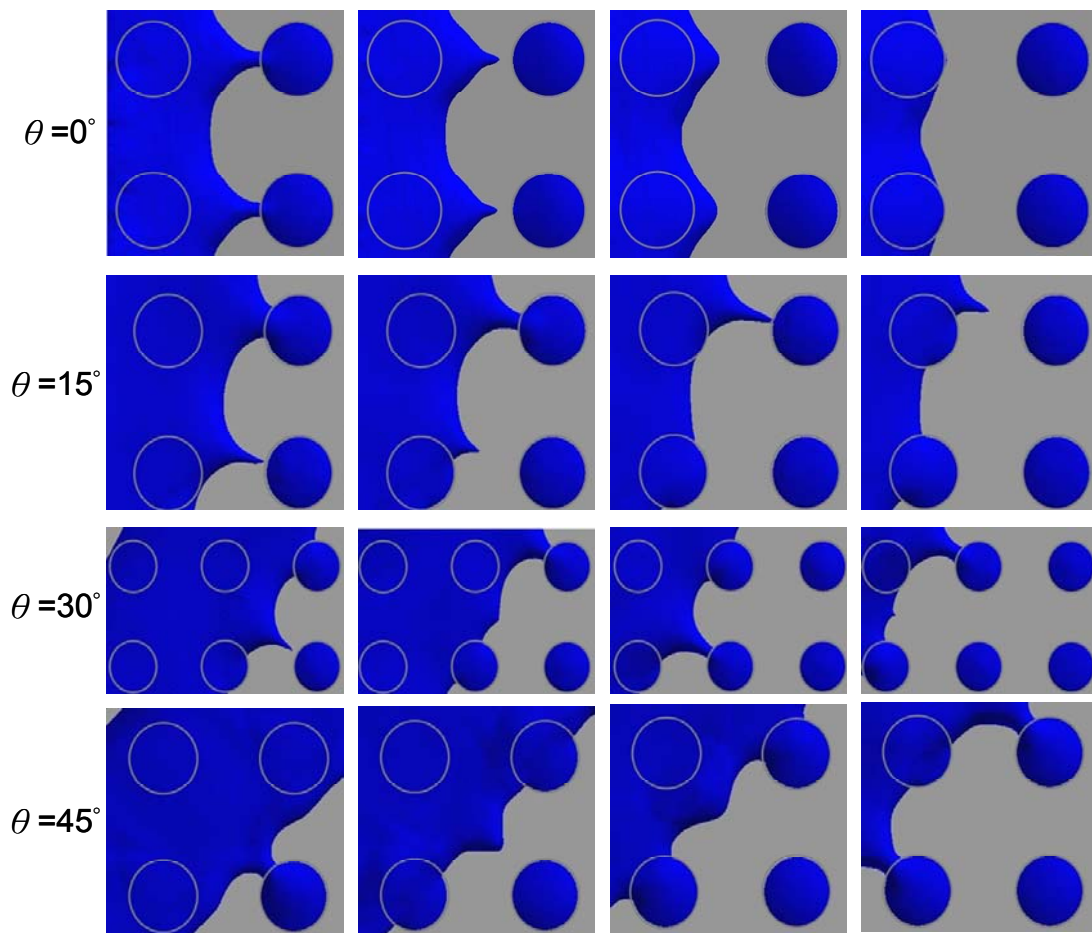
Figure 4. The top views of the calculated dewetting free surface profiles at different peeling angles.

Figure 5 gives the comparison of measured and calculated DNA nanostrand trajectory obtained from the dewetting process on microwells at different peeling angles, where the hollow symbols show the variation of experimental measurements and solid ones represent the calculated results. Our numerical prediction has good agreement with measured results. Akin to the experimental observation, the trajectory of DNA nanostrands at the peeling angle of 30° clearly gives a critical point, where the trajectory changes its tangent direction. This is explained by the vanishing of the local tail-like front during the dewetting process, which is followed by a locally concave water front. The occurrence of concave water front avoids the other end of DNA nanostrands from immobilizing at the edges of the microwells horizontally or diagonally next to the one, where one end of DNA nanostrands has been immobilized there. The longest DNA nanostrands are therefore resulted, as the DNA nanostrands are finally immobilized at the edge of the microwell two-row horizontally and one-row vertically away from the focused microwell. Our numerical simulations successfully explain the mechanism of highly-ordered DNA patterning by dewetting process on microwells.
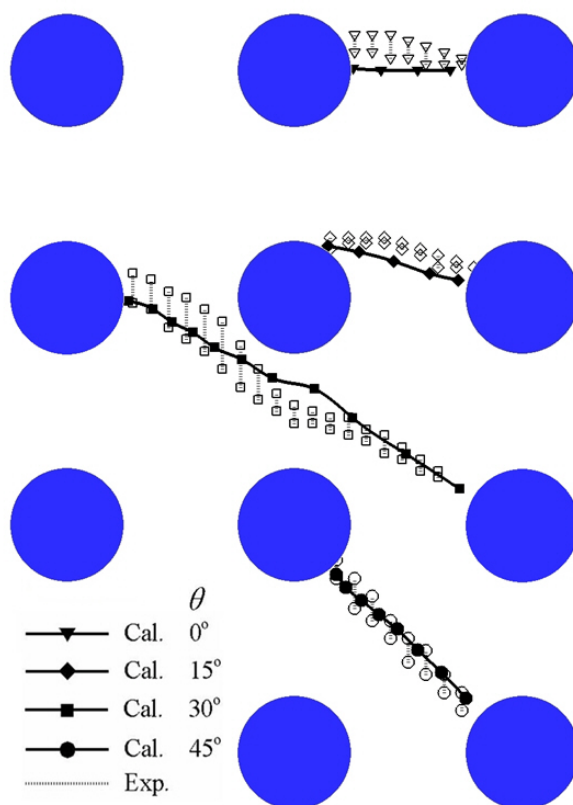
Figure 5. Comparison of measured and calculated DNA nanostrand trajectory obtained from the dewetting process on microwells at different peeling angles.

Conclusion

In this work, a simulation work is shown to help understand the physical process of DNA stretching process. From the simulation results, we can easily know why and how DNA can be stretched and immobilized in a highly ordered pattern. For different peeling angles,

the calculated free surface profile movements can be used to predict the direction of DNA to be stretched. However, in the simulation, only the flow field is calculated. There is no coupled DNA molecules dynamics. In the future, the Brownian dynamics simulation for DNA will be integrated in the simulation.

Literatures

1. Guan, J.J. and J. Lee, *Generating highly ordered DNA nanostrand arrays.* Proceedings of the National Academy of Sciences of the United States of America, 2005. **102**(51): p. 18321-18325.

2. Perić, M. and Ferziger, J.H., Computational Methods for Fluid Dynamics, Springer Verlag, 1996.

3. Brackbill, J.U., Kothe, D.B. and Zemach C., *A Continuum method for modeling surface tension*, J. Comp. Physics, 1992, **100**, p. 335-354.